Available online at www.sciencedirect.com
ScienceDirect
Journal of Power Sources 174 (2007) 124–135
JOURNAL OF POWER SOURCES
www.elsevier.com/locate/jpowsour

Performance analysis of the SOFC–MGT hybrid system with gasified biomass fuel

Made Sucipta [a,*], Shinji Kimijima [b], Kenjiro Suzuki [a,b]

[a] *Graduate School of Engineering, Shibaura Institute of Technology, 307 Fukasaku, Saitama 337-8570, Japan*
[b] *Department of Machinery and Control System, Shibaura Institute of Technology, 307 Fukasaku, Saitama 337-8570, Japan*

Received 25 June 2007; received in revised form 20 August 2007; accepted 28 August 2007
Available online 6 September 2007

Abstract

Analysis of electricity generation efficiency of the biomass SOFC–MGT hybrid system has been made for several cases of different composition of fuel relevant to typical air-, oxygen- and steam-blown biomass gasification processes. Reference case for comparison is the one where pure methane is used as fuel. In the analysis, multi-stage model for internal reforming SOFC module developed previously has been used with some modification. It is found that efficiency achieved for all the three cases of different types for biomass fuel is reasonably high and so that the biomass SOFC–MGT hybrid system is promising. However, in all the three cases, efficiency is lower than the counterpart of pure methane case, both in the SOFC module and in the hybrid system. Among the biomass fuel cases, efficiency is found to be highest with steam-blown biomass fuel both for the SOFC module and for the hybrid system. The lowest efficiency is found in the case of air-blown fuel. In addition, effects of higher steam content in the biomass fuel and variety in composition of biomass fuel for each gasifying agent are also studied.

Keywords: Efficiency analysis; Biomass; Gasification; Gasifying agent; SOFC–MGT hybrid system

1. Introduction

Biomass is widely recognized as one of the promising renewable energy resources and is characterized by zero CO_2 net emission rate and low SO_2 emission rate [1]. There are several technologies to produce fuel for power generation from biomass such as fermentation, combustion, pyrolysis and gasification [2]. Among others, gasification is considered to be the most attractive technology to utilize biomass for energy purposes, because this technology can result in lower pollutant emission rate compared to the combustion technology. In addition, gasification process can produce much higher volume of gas compared to the pyrolysis [3].

Gasification is a well-known technology which can be classified depending on the gasifier type, its operating condition, gasifying agent, etc. Air, oxygen and steam are usually used either individually or mixed as a gasifying agent in the most of biomass gasification processes. Generally, biomass fuel produced by fuel production processes contains hydrogen (H_2), carbon monoxide (CO), carbon dioxide (CO_2), water (H_2O), nitrogen (N_2), methane (CH_4) and other heavier hydrocarbons and minor components. Different gasifying agent used in the gasification process will result in different gas composition and quality of the produced biomass fuel.

For example, in dry basis, with air-blown gasification process, produced gas normally contains nitrogen high in concentration [4–7]. With oxygen-blown gasification process, carbon monoxide and/or carbon dioxide are found high in concentration [6,8]. With steam-blown gasification process, produced gas contains hydrogen high in concentration [3,7,9–12]. In addition, regarding the heating value of produced gas, air-blown gasification process produces a lower quality of the gas. However, with oxygen- or steam-blown gasification process, produced gas has higher quality [2,11].

Range for mole concentration variation of the main components in the produced gas (dry basis) is shown in Table 1 [3–12]. With oxygen or steam as a gasifying agent, a small

* Corresponding author. Present address: Department of Mechanical Engineering, University of Udayana, Bukit Jimbaran, Badung, 80361, Bali, Indonesia. Tel.: +62 361 703321; fax: +62 361 703321.
E-mail address: m.sucipta@gmail.com (M. Sucipta).

0378-7753/$ – see front matter © 2007 Elsevier B.V. All rights reserved.
doi:10.1016/j.jpowsour.2007.08.102

Nomenclature

A	active area (m^2)
E	activation energy ($kJ\,mol^{-1}$)
F	Faraday constant ($96{,}485\,C\,mol^{-1}$)
$\bar{g}$	molar Gibbs free energy ($kJ\,kmol^{-1}$)
I	electric current (A)
j	current density ($A\,m^{-2}$)
k	pre-exponential factor ($mol\,m^{-2}\,bar^{-1}\,s^{-1}$)
LHV	lower heating value ($kJ\,kmol^{-1}$)
$\dot{m}$	mass flow rate ($kg\,s^{-1}$)
$\dot{n}$	molar flow rate ($kmol\,s^{-1}$)
p	pressure (kPa)
$\dot{r}$	reaction rate ($kmol\,s^{-1}$)
R	universal gas constant ($8.31434\,J\,mol^{-1}\,K^{-1}$)
RR	recirculation ratio
SCR	steam-carbon ratio
T	temperature (K or °C)
U	utilization factor
V	voltage (V)
$\dot{W}$	electric power (kW)
z	consumption rate ($kmol\,s^{-1}$)

Greek symbols

Δ	difference
η	efficiency

Subscripts

0	standard state of each condition
act	activation
c	cell
Cf	fuel compressor
f	fuel
FC	fuel cell
loss	losses
max	maximum
MGT	micro gas turbine
oc	open circuit
ohm	ohmic
SYS	hybrid system

portion of nitrogen is also found in produced gas. This is because nitrogen is used to facilitate biomass feeding and to avoid back flow of the gas from the gasifier to the feeding unit. In this study, hydrocarbons heavier than methane are artificially treated as methane. This does not produce any serious misleading result because they are normally minor in concentration.

Table 1
Ranges of gas composition (dry basis) of biomass gasified fuel

Composition (mol%)	Gasifying agent		
	Air-blown	O_2-blown	H_2O-blown
CH_4	2–9	6–19	4–14
H_2	5–16	8–32	21–56
CO	8–22	17–43	10–41
CO_2	9–20	21–61	13–27
N_2	42–66	1–5	1–5

Availability of the biomass resources is localized or even clustered in specific regions. Therefore, distributed power generation system is an appropriate choice for end-use applications of biomass fuel. Most of gasifiers operating for power generation are combined today either with gas engine or with gas turbine due to their advantage in efficiency compared to the direct heating with combustion process. However, this efficiency is not high enough compared with the advanced power generation system. Therefore, coupling the biomass energy conversion system to higher performance power generation system such as fuel cell should be more attractive in its performance [13].

Solid oxide fuel cell (SOFC), one of high-temperature fuel cells, has fuel flexibility. In addition to hydrogen, carbon monoxide and various types of hydrocarbons can be used as fuel in principle. As for the rejected heat, exhaust gas temperature is sufficiently high to drive gas turbine if the system is operated at an elevated pressure. Furthermore, because of high fuel cell operating temperature, internal fuel reforming can be introduced. In addition, SOFC–MGT hybrid system of fusing SOFC module to micro gas turbine (MGT) has high electricity generation efficiency compared to the efficiency of the single-used gas turbine. Therefore, biomass fuelled SOFC–MGT hybrid system can be considered as the most promising distributed power generation unit due to its high energy conversion efficiency, fuel flexibility and very low pollutant emission rate.

In recent years, several theoretical studies and field demonstration have been made for SOFC–MGT hybrid system but the fuel considered was natural gas or methane [14–22]. Some feasibility studies also consider biomass fuel as fuel for SOFC–MGT hybrid system [12]. However, discussion was developed only for the case with steam-blown biomass fuel. In addition, the lumped model used for the SOFC stack module is simple and cannot give detailed information about spatial distributions of temperature, species concentration or other quantities existing in the SOFC stack module. Such information is effective in the detailed discussion of the effects of some parameters including the difference in fuel composition to be discussed in this study as will be seen later.

In the present study, performance analysis of SOFC–MGT hybrid system is made for a variety of fuels including the fuels of typical composition to be produced either by using air, oxygen or steam as a gasifying agent. In the study, a multi-stage model is used to describe the processes in internal reforming SOFC stack module with some modification. The model was previously developed [14,15] for the analysis of the efficiency of methane-fuelled SOFC–MGT hybrid system operated at off-design conditions and has been demonstrated to be effective. Attention is particularly paid to the effects of the variety of composition of the fuel. Biomass fuel produced from gasification process usually contains some impurities [6]. In this study, biomass fuel to be used in the SOFC–MGT hybrid system is assumed to be clean in a sense that the raw fuel produced in the gasifier has been processed in the purifier to

remove impurities. However, details of biomass gasification processes and biomass fuel purification are not discussed in this study.

2. Mathematical model

2.1. Basic assumptions

SOFC module to be studied in the present article is the Siemens-Westinghouse type internal reforming one using the stack of tubular SOFC. The following assumptions are introduced to develop its mathematical model:

(1) Fuel supplied to the system is gasified biomass fuels with such compositions as will be described later.
(2) The air supplied to the system is composed of 78.22% N_2, 20.74% O_2, 0.03% CO_2, and 1.01% H_2O in mole.
(3) All chemical species of working fluids are treated as ideal gas.
(4) The electrochemical reactions of both H_2 and CO proceed at the local temperature of each tubular cell.
(5) The operating cell voltage is the same for every tubular cell.

2.2. System configurations

A schematic diagram of the SOFC–MGT hybrid system under investigation is composed of internal reforming tubular SOFC stack module, MGT, an air compressor, a fuel compressor, a combustor, air recuperator and fuel recuperator as is shown in Fig. 1. SOFC stack module in the hybrid system is divided into two parts, namely, stack of tubular SOFC and reformer. A stack of tubular SOFC is composed of tubular cells of 150 cm long and 2.2 cm in diameter [20–22]. Tubular cell is of a cylindrical shell

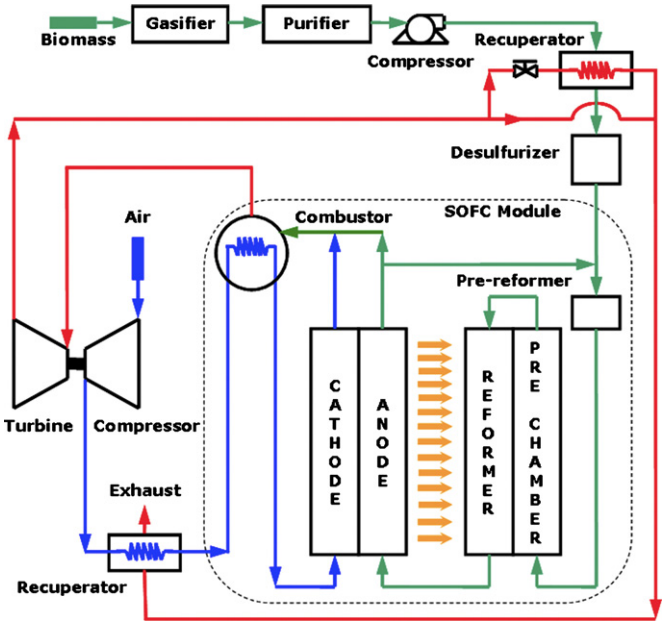

Fig. 1. Schematic diagram of SOFC–MGT hybrid system.

composed of three layers: cathode (inner layer), electrolyte, and anode (outer layer). MGT in the hybrid system is a regenerative turbine.

Compressed fuel is preheated with a portion of the turbine exhaust gas in a fuel recuperator up to an appropriate temperature for desulfurization process in a desulfurizer. Even the sulfur content of biomass fuel is usually very low compared with fossil fuels [2], sulfur can affect the performance of the fuel cell. For example, in the biomass gasification process, concentration of sulfur (H_2S) in the produced gas can be 22 ppm [23]. Addition of 1 ppm H_2S to the fuel (89% H_2 and 11% H_2O) can result in 10% cell voltage drop in SOFC during the first 24 h followed by further drop of voltage then after and this voltage drop can be avoided by removing H_2S from the fuel [22]. H_2S removal can be done through hydro-desulfurization (HDS) process, and the optimum temperature for HDS catalysis is between 350 and 400 °C [24]. In this study, chemical detail of the process is not considered and the temperature of desulfurization process is assumed to be 400 °C. It is found in preliminary calculation that the change of desulfurization temperature from 300 to 400 °C does not affect the performance of the SOFC–MGT hybrid system significantly.

Desulfurized fuel is fed into a pre-reformer after mixing with the recirculated effluent of SOFC. It is partially reformed there utilizing its own internal energy, enters into an indirect internal reformer and then is supplied to the SOFC cell stack. Air is elevated in pressure with a compressor driven by the turbine, and then preheated in the air recuperator by the turbine exhaust gas after heating the fuel. Air is further heated in a heat exchanger mounted in the combustor before entering into the SOFC. Air supplied into the SOFC electrochemically reacts with the fuel supplied to the anode in the tubular SOFC. SOFC module generates main portion of electricity. Effluent from SOFC is burnt in the combustor and expanded in the turbine to produce additional electricity and power to drive air compressor.

2.3. Multi-stage model of SOFC module

Inside the cell stack of SOFC module, fuel flows in a longitudinal direction along the outer surface, i.e. the anode, of each tubular cell. Air is supplied inside the tubular cell through an air feeding tube located at the center of each tubular cell and returns back in a longitudinal direction through the annulus between the air-feed tube and the inner surface of each tubular cell, i.e. the cathode. The electrochemical reaction to occur in the cell is interrelated to the heat generation, heat transfer and mass transfer accompanied with ionic and electric current generation. In this study, all these processes are treated with the previously developed multi-stage model [14,15] with some modification. With this model, whole module is first divided into three zones of different function, pre-chamber, reformer and cell stack with two separating walls, i.e. a reformer wall and a feed plate. Reforming process of hydrocarbons partially occurs in the pre-reformer before entering the module. Fuel is heated in the pre-chamber and reforming process is almost completed in the reformer with the heat supplied from the cell stack. Cell stack

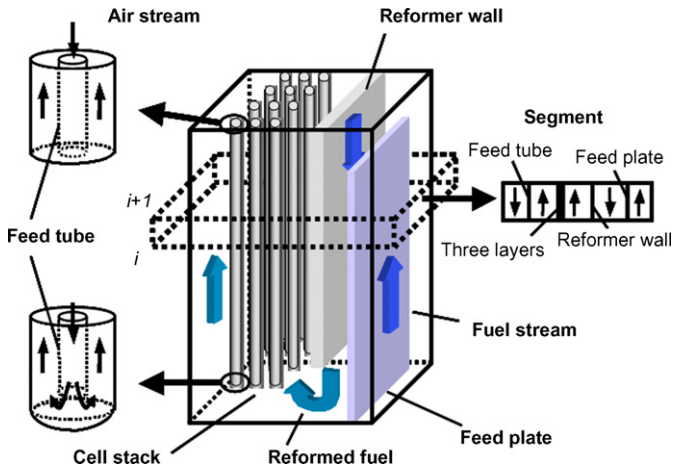

Fig. 2. Multiple segments along the longitudinal direction.

is further divided into three flow spaces, i.e. air flows inside the feed tube and in the annulus inside the cell and fuel flow outside the cell, and two solid phases, i.e. feed tube wall and the cell itself. So totally results in nine regions, namely five flow spaces and four solid parts. The whole region is then sliced into horizontal layers, say N in number. Then, totally, whole module is divided into $9N$ segments, as shown in Fig. 2. Chemical composition and temperature are computed in each segment based on the governing equations for electrochemical and reforming reactions, ionic and electric current and heat generation, heat and mass transfer.

Methane in the fuel is reformed to hydrogen and carbon monoxide through steam reforming processes through the following two chemical reactions:

$$\text{fuel reforming}: \quad CH_4 + H_2O \rightarrow CO + 3H_2 \tag{1}$$

$$\text{shift}: \quad CO + H_2O \leftrightarrow CO_2 + H_2 \tag{2}$$

Shift reaction is fast enough to assume equilibrium and reforming rate is calculated adopting the following model by Achenbach [25]:

$$\dot{r}_{CH_4} = k_{CH_4} p_{CH_4} \exp\left(\frac{-E_{CH_4}}{RT}\right) \tag{3}$$

Both of hydrogen and carbon monoxide thus generated participate in the following overall reaction to proceed electrochemically in SOFC cell stack [26,27]:

$$\text{hydrogen}: \quad H_2 + (1/2)O_2 \rightarrow H_2O \tag{4}$$

$$\text{carbon monoxide}: \quad CO + (1/2)O_2 \rightarrow CO_2 \tag{5}$$

Hydrogen and carbon monoxide are consumed at the rate regulated by electrochemical reactions and directly related to the electricity generation rate. For example, at the air electrode or anode, oxygen is reduced by the following reaction:

$$O_2 + 2e \rightarrow 2O^{2-} \tag{6}$$

and at the fuel electrode or anode, oxygen ion conducted through the electrolyte reacts with hydrogen and carbon monoxide releasing the electrons via following reactions:

$$H_2 + O^{2-} \rightarrow H_2O + 2e \tag{7}$$

$$CO + O^{2-} \rightarrow CO_2 + 2e \tag{8}$$

The released electrons return back to the cathode through external circuit at the rate of current density or at the electricity generation rate. Fuel utilization factor, U_f, is defined as the mole ratio of the consumption rates of hydrogen and carbon monoxide to the supplying rates of methane, carbon monoxide and hydrogen, namely:

$$U_f = \frac{z_{H_2} + z_{CO}}{(4\dot{n}_{CH_4} + \dot{n}_{CO} + \dot{n}_{H_2})_{\text{supplied}}} \tag{9}$$

As shown in Eqs. (1) and (2), steam is a necessary participant in the reforming processes. In fact, the steam-carbon ratio of fuel to be supplied to anode must be an appropriate value to avoid the carbon deposition to the cell. Steam is partially supplied included in fuel in case of biomass fuel but added more by recirculating the effluent from the anode of fuel cell. Recirculation ratio (RR) is defined as the ratio between the recirculated mole flow rate to the total mole flow rate of exhaust gas from the anode and it is related to the steam-carbon ratio (SCR), which is defined as the mole ratio of the steam to the carbon in the supplied fuel as follows:

$$\text{RR} = \frac{\text{SCR}(\dot{n}_{CH_4} + \dot{n}_{CO} + \dot{n}_{CO_2})_{\text{supplied}} - (\dot{n}_{H_2O})_{\text{supplied}}}{(\dot{n}_{H_2O})_{\text{anode channel exit}}} \tag{10}$$

2.4. Lumped model for MGT system

Micro gas turbine to be discussed here is composed of four major components, namely: air compressor, combustor, turbine and recuperator. Air compressor and turbine in the MGT are generally single-stage centrifugal and radial types, respectively, and the lumped model is applied for them in this study. By considering the energy balances in air compressor and turbine with known inlet conditions, the exit conditions can be easily computed with the functions of isentropic efficiencies. In the present study, overall fuel air ratio is controlled to keep the turbine inlet temperature (TIT) of the MGT at a fixed value in all cases. Additional work to drive a fuel compressor $\dot{W}_{Cf}$ is treated in this article separately from the gas turbine network or electricity generation $\dot{W}_{MGT}$. Therefore, the total power of MGT appearing in the discussions to follow is the sum of $\dot{W}_{MGT}$ and $\dot{W}_{Cf}$.

The role of the combustor is to burn the unreacted fuel remaining in the effluent from the anode of the SOFC, namely remaining hydrogen, carbon monoxide and methane. The chemical reactions to occur in the combustor are:

$$\text{hydrogen}: \quad H_2 + (1/2)O_2 \rightarrow H_2O \tag{11}$$

$$\text{carbon monoxide}: \quad CO + (1/2)O_2 \rightarrow CO_2 \tag{12}$$

$$\text{methane}: \quad CH_4 + 2O_2 \rightarrow CO_2 + H_2O \tag{13}$$

Burnt gas in the combustor is first used to heat up the air in the recuperator mounted in the combustor and then supplied to MGT at a temperature meeting the assumed value of TIT.

2.5. System performance

The maximum power to be produced by the electrochemical reaction in the fuel cell, W_{FCmax}, is equal to the change in the Gibbs free energy, $-(z_{H_2} + z_{CO})\Delta\bar{g}$, occurring in the electrochemical reaction at the molar consumption rates z_{H_2} and z_{CO}, respectively for hydrogen and carbon monoxide. Their relationship can be converted to calculate the open-circuit voltage (OCV), V_{oc}, as follows:

$$W_{FCmax} = -(z_{H_2} + z_{CO})\Delta\bar{g} = 2(z_{H_2} + z_{CO})FV_{oc} \quad (14)$$

where F is the Faraday constant. Since the participating chemical gas components are considered to be ideal, the change in the Gibbs free energy per 1 mol of hydrogen can be expressed as:

$$-\Delta\bar{g} = -\Delta\bar{g}^0 + RT\ln\left[\frac{p_{H_2}/p_0(p_{O_2}/p_0)^{1/2}}{p_{H_2O}/p_0}\right] \quad (15)$$

The change of Gibbs free energy per 1 mol of carbon monoxide should be equal to that of hydrogen [25] under the equilibrium assumed for the shift reaction. This means that the OCV is the same both for hydrogen and carbon monoxide.

Defining the current density, j, as the transfer rate of ionic charge per unit effective area of the fuel cell, the electric power to be produced in the fuel cell can be expressed as:

$$W_{FC} = V_c j A_c \quad (16)$$

The cell voltage, V_c, in operation differs from the open-circuit voltage by total over-potential or the voltage losses to occur due to the irreversible processes in the fuel cell, i.e.:

$$V_c = V_{oc} - \Delta V_{loss} \quad (17)$$

where ΔV_{loss} is the sum of the activation, ohmic and concentration over-potentials. In the present study, only the activation and ohmic losses, ΔV_{act} and ΔV_{ohm}, are taken into consideration:

$$\Delta V_{loss} = \Delta V_{act} + \Delta V_{ohm} \quad (18)$$

The empirical equations by Achenbach [25] are adopted for the activation polarization. The ohmic losses in the tubular SOFC are considered not only for radial ionic current across the electrolyte, but also for circumferential electric current through the anode and cathode. Detailed empirical formulas of the over-potential can be found in Refs. [17,25].

In the following, electricity generation efficiency will be presented separately for the SOFC module of the system and for the SOFC–MGT hybrid system for the convenience of discussion. They are defined, respectively, as follows:

$$\eta_{FC} = \frac{\dot{W}_{FC}}{\dot{m}_f LHV_f} \quad (19)$$

$$\eta_{SYS} = \frac{\dot{W}_{FC} + \dot{W}_{MGT} - \dot{W}_{Cf}}{\dot{m}_f LHV_f} \quad (20)$$

where LHV_f is the lower heating value of fuel.

Table 2
Typical gas composition (dry basis) considered as fuel in this study

Composition (mol%)	Pure methane	Gasifying agent		
		Air-blown	O_2-blown	H_2O-blown
CH_4	100	5	10	10
H_2	–	10	20	40
CO	–	15	30	25
CO_2	–	15	35	20
N_2	–	55	5	5
LHV (kJ kg^{-1})	50,019	3911	7843	12,624

3. Results and discussions

In the following, comparison will first be made among the three cases of dry gasified biomass fuel with typical compositions to be produced with different gasifying agents, i.e. steam, oxygen and air. The fuel compositions are shown in Table 2 and pure methane case is included as a reference for comparison, of which results have been presented elsewhere [28].

Steam is included sometimes high in concentration in the gasified biomass fuel [7] depending on the specific gasification process to be adopted. For example, difference exists just between dry biomass fuel and wet biomass fuel. In case of dry biomass fuel, water is condensed after the purifier at an appropriate temperature and then heated up to a pre-specified temperature before entering into the fuel compressor in the system. In case of wet biomass fuel, fuel is directly cooled down after the purifier to the same pre-specified temperature without condensing water. Therefore, steam content is higher in the latter case. Steam concentration of the gasified biomass fuel depends certainly on the kind of gasifying agent, on the type of the gasifier, and on the type and moisture level of biomass resources as well. Thus, concentration of water in the biomass fuel varies case by case. Therefore, effects of the steam concentration in fuel will be discussed next in this article. To cover the wet biomass fuels, steam is increased up to 40% in mole concentration.

Lastly, discussion will also be developed for the effects of further modification of fuel composition. This is based on the fact that chemical composition of biomass fuel is diversified as already discussed with Table 1 even among the cases using the same gasifying agent.

3.1. Performance of the SOFC–MGT hybrid system with dry biomass fuel

The condition for the present performance analysis of a tubular SOFC–MGT hybrid system is given in Table 3. Most of the data tabulated in Table 3 are based on the published data [20–22]. Some of those values, including compressor and turbine efficiencies, were assumed considering their current general performance trends. As seen in Table 3, all of the net total power to be produced, turbine inlet temperature and averaged current density are fixed as constant. This gives simpler background for the discussion of the effect of the different composition of the gasified biomass fuel. However, one point to be noticed is that the effective cell area is adjusted to keep the total power to be

Table 3
Physical conditions for the performance analysis

System	
Net total power (kW)	220
Ambient conditions	25 °C, 1 atm
Fuel cell	
Steam-carbon ratio	2.5
Fuel utilization factor	0.85
Average current density (A m^{-2})	3200
Fuel inlet temperature (°C)	150
Gas turbine	
Pressure ratio	2.9
Turbine inlet temperature (°C)	840
Compressor adiabatic efficiency (%)	78
Turbine adiabatic efficiency (%)	82
Recuperator effectiveness (%)	89
Geometry of tubular SOFC	
Cathode thickness (mm)	2
Electrolyte thickness (μm)	40
Anode thickness (μm)	125
Interconnector thickness (μm)	100

produced. In this relation, ratio of the power to be obtained, respectively, with SOFC module and that with MGT is automatically changed, as will be discussed later.

It is important to note that efficiency achieved for all the three cases of different types of biomass fuel is reasonably high and so that the biomass SOFC–MGT hybrid system is feasible. However, in all the three cases, efficiency is lower than the counterpart of pure methane case, both for the SOFC and for the hybrid system, as shown in Fig. 3 (at 0% H_2O concentration). This is mainly due to the lower heating value of biomass fuel and the effect of inactive species existing in biomass fuel at a certain concentration (see Table 2). For the same reason, among the three cases of different biomass fuel, efficiency is found to be highest with steam-blown biomass fuel both for the SOFC module and for the hybrid system, i.e. for example efficiency is 38.0% for the SOFC module and 50.8% for the hybrid system, respectively, in that case. With oxygen-blown fuel, the efficiency is 35.9% and 48.9% for SOFC module and hybrid system, respectively. The lowest efficiency is found in the case of air-blown fuel, i.e. the efficiency of the SOFC module being 34.9% and the efficiency of the hybrid system 46.4%.

As has been listed in Table 3, the net total power or electricity generation and the averaged current density are fixed in the computation. Therefore, the active cell area of the SOFC or total electric current to be produced is automatically adjusted in the calculation. For example, in the pure methane case, total electric current is calculated to be 306.2 kA, as found in Fig. 4. However, with air-blown biomass fuel, total electric current is highest among all the studied cases, i.e. 331.0 kA. With oxygen-blown fuel, the electric current is found to be 314.5 kA. With steam-blown fuel, 304.1 kA is enough for electric current and it is smallest among the three cases. These results indicate that the necessary cell active area is largest for air-blown biomass fuel. Namely, it is 103.4 m^2 for air-blown biomass fuel, 98.3 m^2 with oxygen-blown fuel, and 95.0 m^2 with steam-blown fuel.

Highest total electric current found in air-blown fuel case results in the largest power produced by SOFC module among the three biomass fuel cases. It may be valuable, however, to note that the produced power is still lower than that of pure methane case. This is related to the low operating cell voltage. As is found in Fig. 4, with air-blown biomass fuel, operating cell voltage is 0.526 V, with oxygen- and steam-blown fuel the cell voltages are 0.541 and 0.569 V, respectively. The lowest cell voltage basically comes from the lowest concentration of H_2 and CO, the effective fuel, in the inlet of the cell or in the

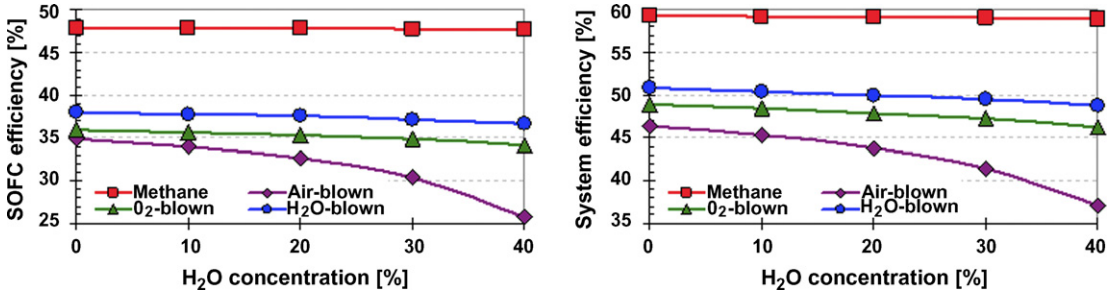

Fig. 3. Changes of efficiency of the SOFC and of the hybrid system.

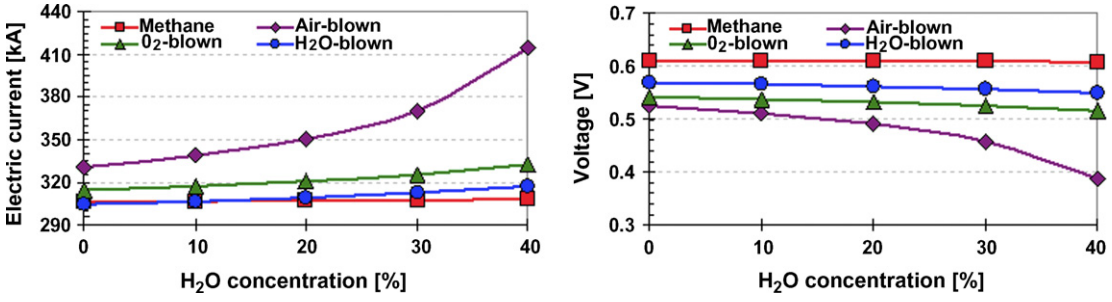

Fig. 4. Changes of total electric current and operating cell voltage.

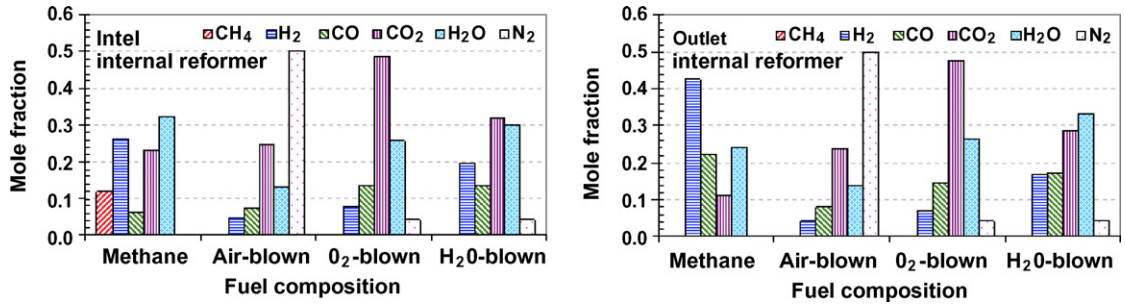

Fig. 5. Concentration distribution of gas in the internal reformer for dry biomass fuel.

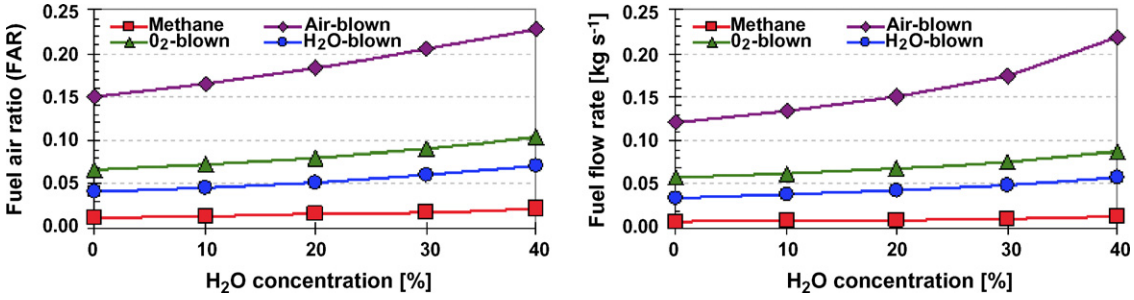

Fig. 6. Changes of fuel air ratio and fuel flow rate.

outlet of internal reformer, as shown in Fig. 5. It is concluded that cell voltage tends to increase with an increase of H_2 and CO concentration at the inlet of the cell.

In this study, fuel air ratio is automatically adjusted to keep TIT constant at 840 °C. In all the gasified biomass fuel cases, the heating value of fuel is lower compared to that of pure methane as has been mentioned above. This indicates that SOFC power generation tends to decrease unless the fuel flow rate is increased and combustor outlet temperature tends to decrease unless the fuel air ratio is increased. Therefore, larger fuel air ratio and larger fuel flow rate must be introduced to keep both TIT and net total power generation constant. This is confirmed in Fig. 6.

In air-blown biomass fuel case, higher flow rate of fuel means the necessity of larger power to drive the fuel compressor, therefore to meet this, larger MGT power and SOFC power to be generated. For example, with air-blown fuel, the power produced by the SOFC and the one by the MGT are 165.3 and 79.3 kW, respectively, as shown in Fig. 7. With oxygen-blown fuel, SOFC power is 161.8 kW and MGT power is 69.7 kW. With steam-blown fuel, they are found to be 164.4 and 65.2 kW, respectively.

It is interesting to note that averaged cell temperature is a little higher in the cases of the oxygen- and steam-blown biomass fuel compared to the case of air-blown biomass fuel or even compared to the pure methane case, as is shown in Fig. 8. Compared to the pure methane case, necessary heat to support the steam reforming process in the internal reformer is smaller in those two cases because of smaller methane concentration in the fuel even if fuel flow rate is larger. Reforming of methane is treated in this study to proceed up to a certain degree in the pre-reformer and concentration of methane is already low at the inlet to the reformer, as is seen in Fig. 5. However, lower heat transfer rate from the cell to the reformer wall to support milder reforming process is countered by the larger flow rate of air, the cell coolant, in the cases of the oxygen- and steam-blown biomass fuel, as shown in Fig. 8. This results in only a little higher averaged cell temperature in case of oxygen- and steam-blown biomass fuel. This heat transfer trends are confirmed in Fig. 9.

As is found in Fig. 10, in all the three cases of biomass fuel, gas temperature distribution in the internal reformer becomes flatter than in the pure methane case. Similar tendency is found in Fig. 11 for the reformer wall temperature and for the cell temper-

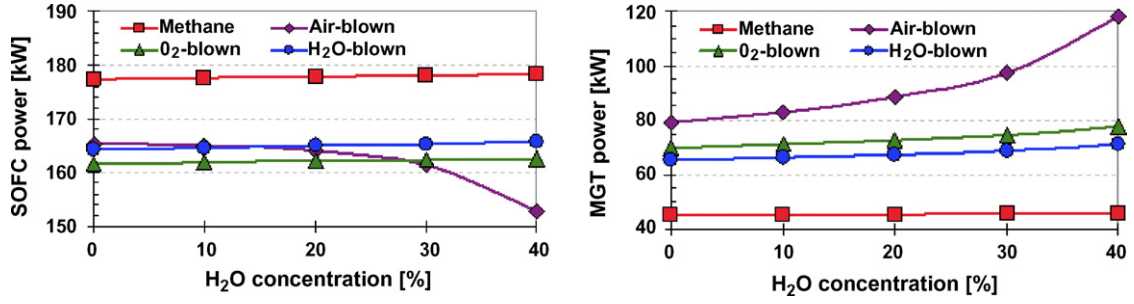

Fig. 7. Changes of power produced by the SOFC module and by the MGT.

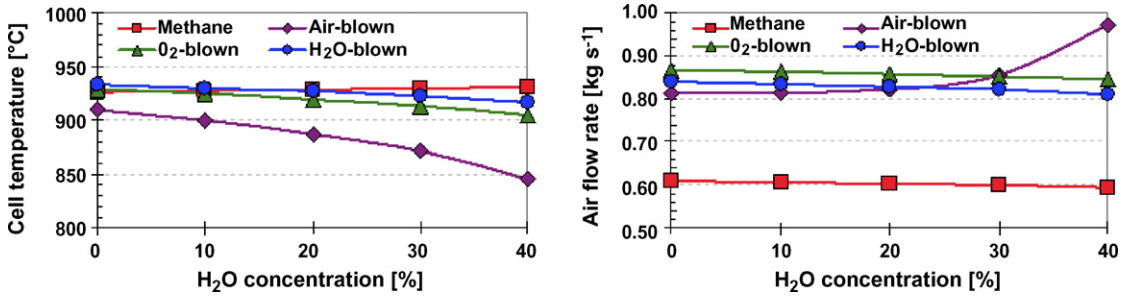

Fig. 8. Changes of averaged temperature of the cell of SOFC and air flow rate.

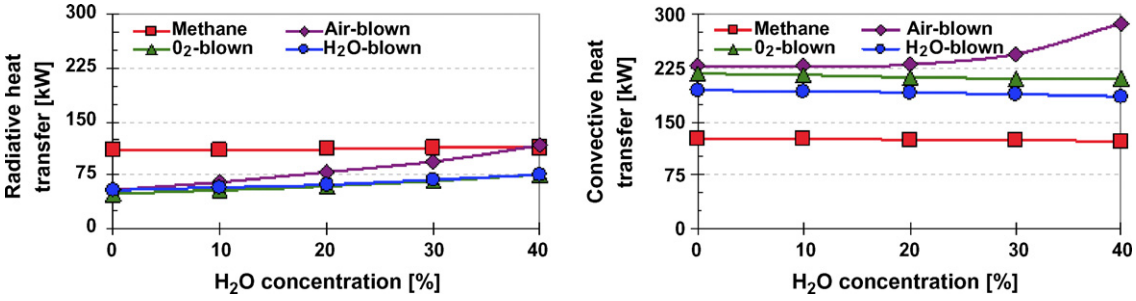

Fig. 9. Changes of radiative and convective heat transfer rate in the SOFC module.

ature. This means temperature difference between the cell stack and reformer is smaller. This is due to the fact that lower heat transfer rate is enough to support endothermic reforming reaction of methane of lower concentration in biomass fuel cases.

3.2. *Effects of the steam content in wet biomass fuel*

Now the effects of the steam concentration in the wet biomass fuel are studied. Addition of steam to 50% in mole concentration has been found not to result in any significant change in the efficiency when it is mixed to pure methane [28]. However, this is not the case where steam is added to biomass fuel. If steam is added up to 40% in concentration in case of biomass fuel, performance of the SOFC–MGT hybrid system can change significantly as is seen in Fig. 3. For example, with wet air-blown biomass fuel having 40% steam concentration, efficiency of the SOFC decreases from 34.9 to 25.7% and efficiency of the hybrid system from 46.4 to 37.0%. However, drop in efficiency is not always so significant. In case of wet oxygen-blown fuel, efficiency of the SOFC decreases from 35.9 to 34.2% and efficiency

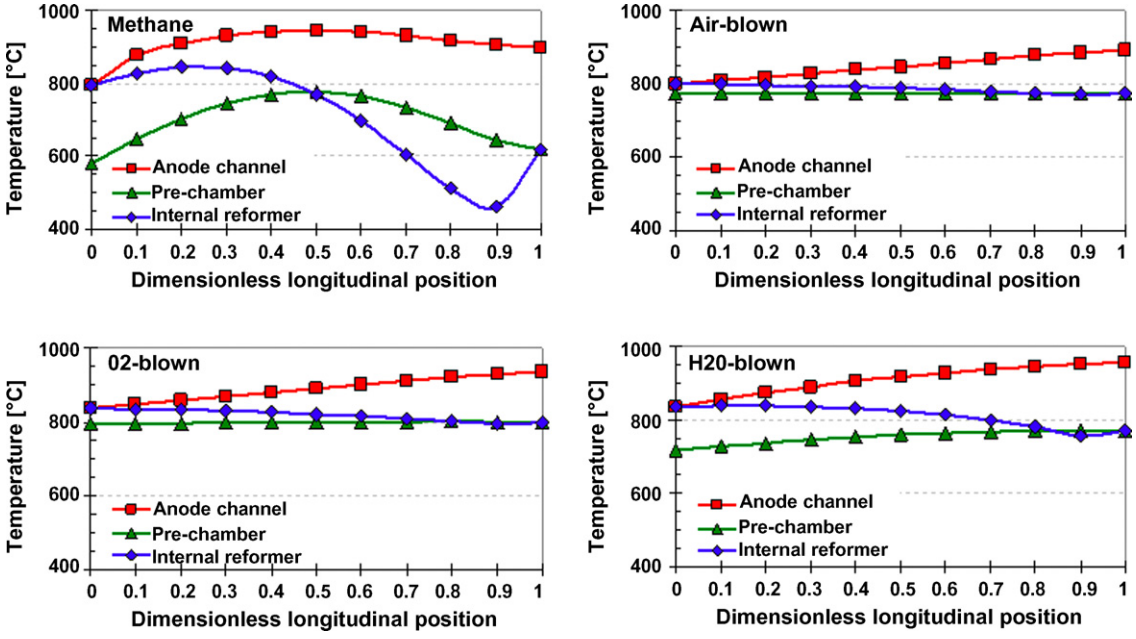

Fig. 10. Temperature distribution of fuel in the SOFC module.

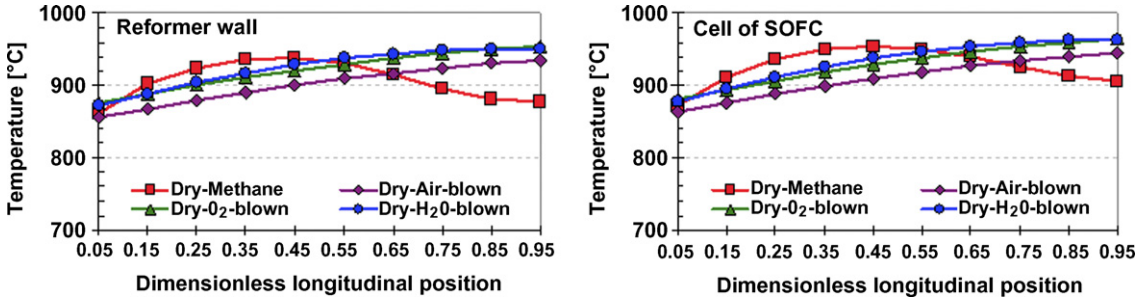

Fig. 11. Temperature distribution of solid along the longitudinal direction of SOFC for dry biomass fuel.

of the hybrid system decreases from 48.9 to 46.2%, respectively. In case of wet steam-blown fuel, efficiency of the SOFC module decreases from 38.0 to 36.7% and efficiency of the hybrid system from 50.8 to 48.8%. This reduction of the efficiency accompanying the steam addition is caused by the decrease of heating value of the fuel.

As discussed above, fuel flow rate and fuel air ratio should be increased to keep both TIT and the net total power generation constant to counter the lower value of fuel heating value caused by an increase of steam concentration in the wet biomass fuel. With wet air-blown biomass fuel, SOFC power decreases from 165.3 to 152.8 kW but MGT power dramatically increases from 79.3 to 118.3 kW to supply the fuel compressor power increased with an increase of steam mole concentration from 0 to 40% as is confirmed in Fig. 7. On the other hand, change is not so dramatic in other two cases of the wet oxygen-blown and wet steam-blown biomass fuels; namely in the former case, an increase of the power of SOFC module is from 161.8 to 162.5 kW and the one of MGT is from 69.7 to 77.7 kW and in the latter case, change of the SOFC module power and MGT power from 164.4 to 165.8 kW and from 65.2 to 70.9 kW, respectively.

As is seen in Fig. 4, in case of wet air-blown biomass fuel, with an addition of steam mole concentration up to 40%, a significant increase of total electric current is required to keep the total power and electric current density constant, i.e. the total electric current is 414.9 kA and 129.7 m^2 is necessary for the cell active area. With wet oxygen- and steam-blown fuel, the cell active area is 103.9 and 99.0 m^2, respectively. On the other hand, a significant decrease of cell voltage is observed with wet biomass fuel in the same figure. For example, with wet air-blown biomass fuel, cell voltage is 0.388 V and with wet oxygen- and steam-blown fuel, cell voltages are 0.515 and 0.551 V. This basically comes from the decreases of heating value and Gibbs free energy of the fuel.

Increasing the steam concentration in the biomass fuel, reduction of the recirculation ratio is needed to keep the steam-carbon ratio in the cell stack constant. This results in the decrease of the gas temperature at the inlet of the internal reformer as shown in Fig. 12. This is an important secondary effect of the effect of steam concentration to be considered.

Methane concentration decreases in wet biomass fuel. However, increase of fuel flow rate and decrease of the gas temperature at the inlet of the internal reformer result in an increase of radiative heat transfer rate from the cell to the reformer wall. These are confirmed in Fig. 9. Accompanying these conditions, averaged cell temperature are found to decrease in all wet biomass fuel cases as is confirmed in Fig. 8. In case of wet air-blown biomass fuel, the largest decrease of averaged cell temperature is observed; i.e. averaged cell temperature being 845.0 °C. Averaged cell temperatures are found to be 904.5 and 917.1 °C, respectively for the cases of wet oxygen- and steam-blown fuels.

3.3. Effect of the species concentration

As is found in Table 1, three types of gasified biomass fuels are different from each other in what species are rich in concentration and in how large the variation range of each species is. In this relation, it may be worth further to study the effects of the difference in the fuel composition. Therefore, performance analysis has been made for totally nine cases of different fuel compositions, 1A–3A, 1O–3O and 1S–3S, tabulated in Table 4. Bold letter cases in the table are the cases of which results have been discussed already in the previous sections. For air-blown

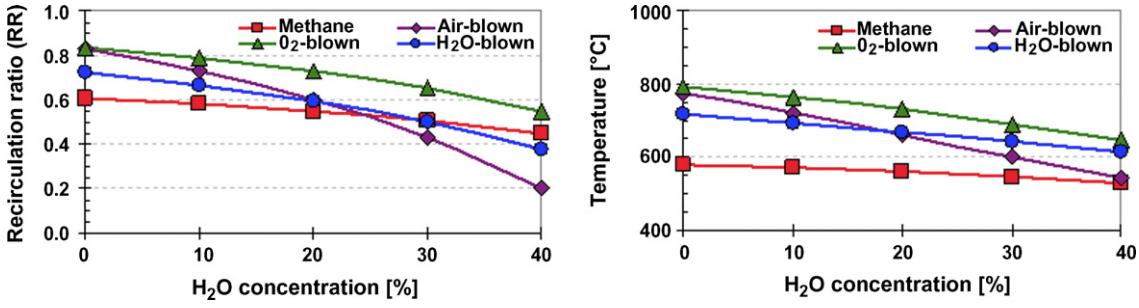

Fig. 12. Changes of recirculation ratio and inlet gas temperature to the internal reformer.

Table 4
Fuel composition of each gasifying agent

Composition (mol%)	Air-blown case			O_2-blown case			H_2O-blown case		
	1A	**2A**	3A	1O	**2O**	3O	1S	**2S**	3S
CH_4	5	**5**	5	10	**10**	10	10	**10**	10
H_2	10	**10**	10	20	**20**	20	30	**40**	50
CO	10	**15**	20	20	**30**	40	35	**25**	15
CO_2	10	**15**	20	45	**35**	25	20	**20**	20
N_2	65	**55**	45	5	**5**	5	5	**5**	5
LHV (kJ kg^{-1})	3493	3911	4306	6426	7843	9437	11,332	12,624	14,309

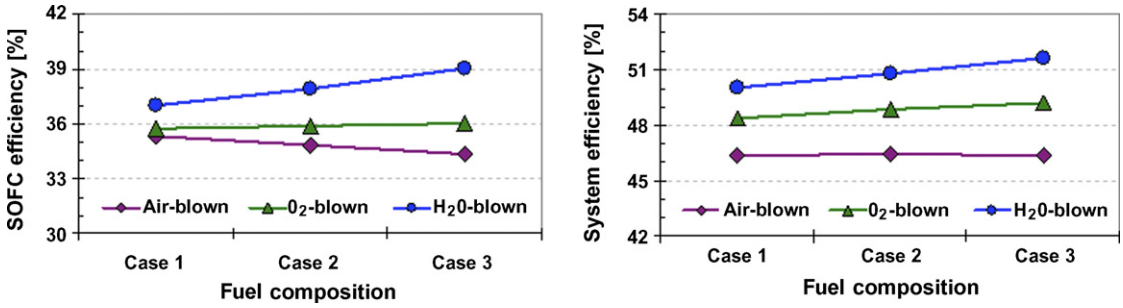

Fig. 13. Changes of efficiency of SOFC module and of hybrid system for all cases.

biomass fuel, N_2 concentration is changed with compensation by the change in CO and CO_2 concentration. For O_2-blown biomass fuel, CO concentration is changed compensating the change in CO_2 concentration and for steam-blown biomass fuel H_2 concentration is changed accompanying the change in CO concentration.

It is found in Fig. 13 that the change of compositions does not significantly affect either SOFC efficiency or hybrid system efficiency in the cases of air- and oxygen-blown biomass fuels but that, in the case of steam-blown biomass fuel, both efficiencies are noticeably changed. Efficiency of SOFC and the one of hybrid system, respectively increase from 37.0 to 39.0%, and from 50.1 to 51.6% between case 1S and case 3S. This is due to the increase of H_2 concentration replacing the CO concentration. CO is fuel but its heating value per unit mass is lower than that of H_2.

Efficiency rise in the steam-blown biomass fuel cases 1S, 2S and 3S resulting from the increase of heating value does not need to accompany the increase of active cell area. Conforming with this, both of total electric current and cell voltage weakly increase. This is confirmed by almost constant value of total electric current among those three cases in Fig. 14.

However, total electric current or necessary cell active area changes a little more noticeably in other two cases of air- and oxygen-blown biomass fuels. For example, with air-blown biomass fuel, total electric current decreases from 339.8 to 325.2 kA between case 1A and case 3A. With oxygen-blown fuel, change of fuel composition from case 1O to case 3O results in the decrease of total electric current from 325.4 to 306.4 kA.

Change in total electric current results in the similar change of the SOFC power as is seen in Fig. 15. This is because the cell voltage does not change significantly with varying the composition of biomass fuel except for its little increase observed in case of oxygen-blown fuel from 0.526 V in case 1O to 0.553 V in case 3O as is found in Fig. 15. Small increase of cell voltage in this case brings about less significant decrease of the SOFC power different from the air-blown fuel case.

As has been discussed above, effects of the fuel composition can be explained mostly with the change in heating value of fuel, heat supplying rate needed in fuel reforming and concentration

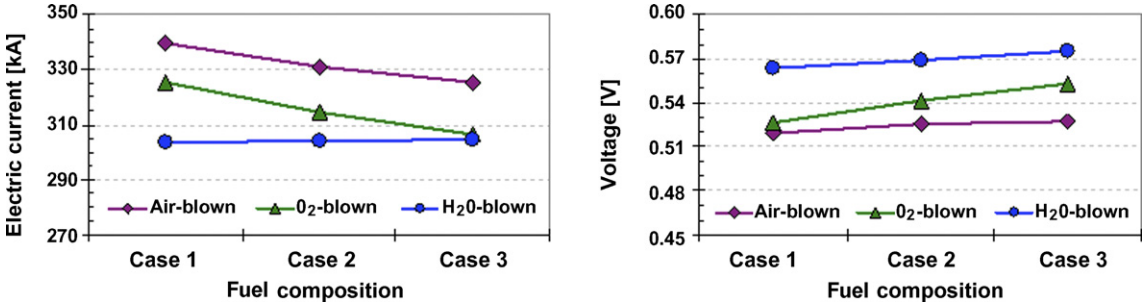

Fig. 14. Changes of total electric current and operating cell voltage for all cases.

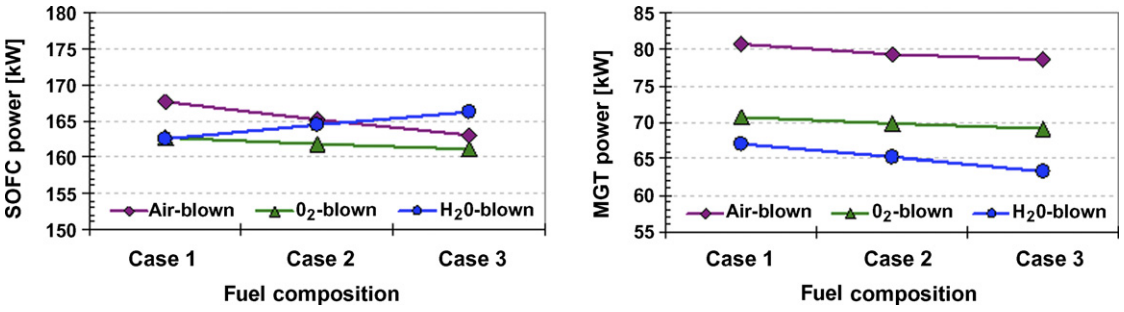

Fig. 15. Changes of power produced by SOFC module and by MGT for all cases.

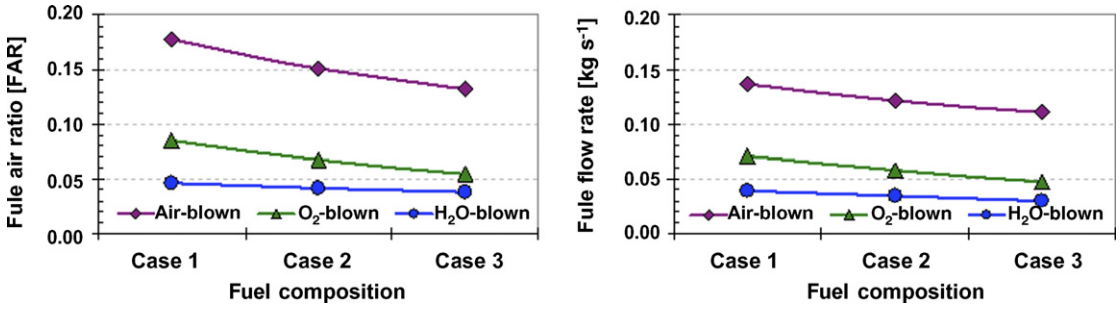

Fig. 16. Changes of fuel air ratio and fuel flow rate for all cases.

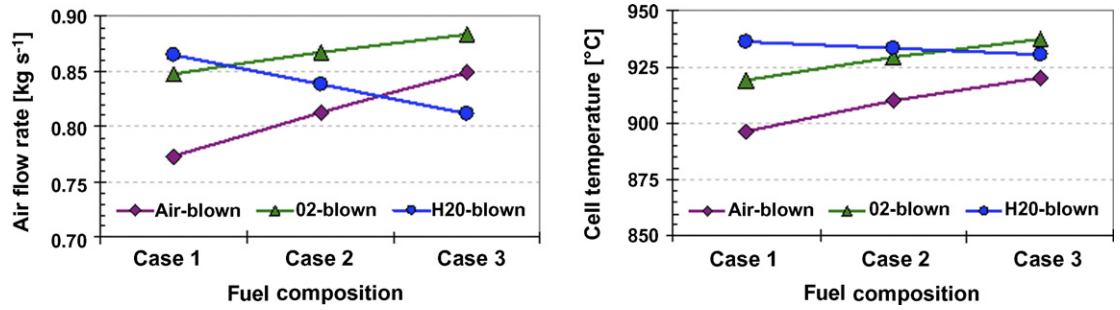

Fig. 17. Changes of average cell temperature and air flow rate for all cases.

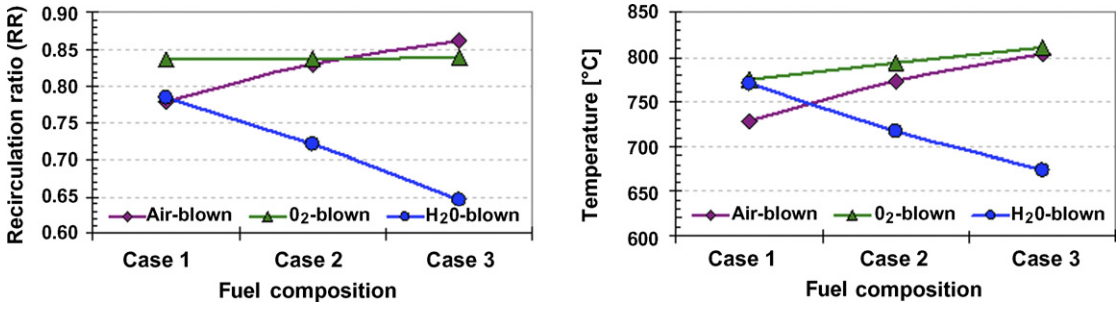

Fig. 18. Changes of recirculation ratio and gas temperature in inlet of internal reformer for all cases.

of non-participating species of fuel relating to fuel heat capacity and fuel compressor power. However, sometimes, more careful discussion is needed to discuss the detail of the results or to see the consistency among all the results. For example, cell temperature increases in case 3A than in case 1A although the flow rate of air, the main coolant, increases. This is related to the change in the recirculation ratio. In case 3A, carbon concentration in fuel is higher than in case 1A so that recirculation ratio is increased to keep the steam-carbon ratio constant. This brings higher fuel temperature at the inlet to the fuel reformer which brings about the higher cell temperature. These are confirmed in Figs. 16–18.

4. Conclusions

Analysis of electricity generation efficiency of the biomass SOFC–MGT hybrid system has been studied for several cases of

different fuel composition relevant to typical air-, oxygen- and steam-blown biomass gasification processes:

(1) In all the studied cases of biomass fuel composition, efficiency is lower than the reference case, both for the SOFC and for the hybrid system. This is mainly due to lower heating value of biomass fuel and the effect of non-participating species existing in biomass fuel. For this reason, efficiency is found to be highest with steam-blown biomass fuel both for the SOFC module and for the hybrid system. Lowest efficiency is found in the case of air-blown biomass fuel.
(2) Mixing of steam to the biomass fuel up to 40% in mole concentration results in the decrease of the efficiency both of the SOFC module and of the hybrid system significantly. The lowest efficiency is also the case of wet air-blown biomass fuel.
(3) An important point to be noted here is that a larger size of hybrid system is needed to produce the same total electricity generation with air-blown biomass fuel, since the lower performance of the SOFC module leads to the necessity of larger cell active area and to the increase in the MGT power.
(4) Further study has been made for the cases of larger variety of fuel composition considering that various fuel compositions are obtained depending on the types of gasification processes, on the kinds of biomass and on the location for biomass plantation. Noticeable change of efficiency is found both for the SOFC module and for the hybrid system with the change of fuel composition in case of steam-blown biomass fuel. On the other hand, change of fuel composition does not affect both the efficiency of the SOFC module and of the hybrid system noticeably in cases of air- or oxygen-blown biomass fuel except for a little change in the necessary cell active area.
(5) Effects of the fuel composition can be explained mostly with the change in heating value of fuel, heat supplying rate needed in fuel reforming and concentration of non-participating species of fuel relating to fuel heat capacity and fuel compressor power. However, to see the consistency among all the results, other parameters like fuel air ratio, fuel flow rate, air flow rate and recirculation ratio relating them have to be paid attention.

Acknowledgements

The present study has partially been supported by the MEXT Grants in Aid for Scientific Research #17360100, the MEXT Academic Frontier Project for SIT Energy Flow Research Center and SIT Project Research Fund for Biomass SOFC. The TPSDP Project of Department of Mechanical Engineering, University of Udayana, Indonesia, is deeply acknowledged for the first author PhD program fellowship.

References

[1] D.J. Stevens, U.S. Department of Energy Report, NREL/TP-421-7501, 1989.
[2] T.B. Reed, A. Das, U.S. Department of Energy Report, SERI/SP-271-3022, 1988.
[3] C. Franco, F. Pinto, I. Gulyurtlu, I. Cabrita, Fuel 82 (2003) 835–842.
[4] I. Narváez, A. Orio, M.P. Aznar, J. Corella, Ind. Eng. Chem. Res. 35 (1996) 2110–2120.
[5] A. van der Drift, J. van Doom, J.B. Vermeulen, Biomass Bioenergy 20 (2001) 45–56.
[6] C.N. Hamelinck, A.P.C. Faaij, H. den Uil, H. Boerrigter, Energy 29 (2004) 1743–1771.
[7] J. Gil, J. Corella, M.P. Aznar, M.A. Caballero, Biomass Bioenergy 17 (1999) 389–403.
[8] J.I. Na, S.J. Park, Y.K. Kim, J.G. Lee, J.H. Kim, Appl. Energy 75 (2003) 275–285.
[9] J. Herguido, J. Corell, J. Gonzalez-Saiz, Ind. Eng. Chem. Res. 5 (1992) 1274–1282.
[10] M. Bolhàr-Nordenkampf, R. Rauch, K. Bosch, C. Aichernig, H. Hofbauer, International Conference on Biomass Utilisation, 2002.
[11] G. Schuster, G. Löffler, K. Weigl, H. Hofbauer, Bioresour. Technol. 77 (2001) 71–79.
[12] T. Proell, R. Rauch, C. Aichernig, H. Hofbauer, ASME Paper GT2004-53900, 2004.
[13] K.R. Craig, M.K. Mann, U.S. Department of Energy Report, NREL/TP-430-21657, 1996.
[14] T.W. Song, PhD Thesis, Seoul National University, 2004.
[15] T.W. Song, J.H. Kim, S.T. Ro, K. Suzuki, ICOPE-3, 2003.
[16] K. Suzuki, T.W. Song, J.H. Kim, S.T. Ro, 59° Congresso ATI, 2004.
[17] T.W. Song, J.L. Sohn, J.H. Kim, T.S. Kim, S.T. Ro, K. Suzuki, J. Power Sources 142 (2005) 30–42.
[18] H. Uechi, S. Kimijima, N. Kasagi, J. Eng. Gas Turbine Power 126 (2004) 755–762.
[19] A.F. Massardo, F. Lubelli, J. Eng. Gas Turbine Power 122 (2000) 27–35.
[20] R.A. George, J. Power Sources 86 (2000) 134–139.
[21] R.A. George, N.F. Bessette, J. Power Sources 71 (1998) 131–137.
[22] S.C. Singhal, Solid State Ionics 135 (2000) 305–313.
[23] A. Corti, L. Lombardi, Energy 29 (2004) 2109–2124.
[24] A.L. Dicks, J. Power Sources 61 (1996) 113–124.
[25] E. Achenbach, J. Power Sources 49 (1994) 333–348.
[26] P.W. Li, K. Suzuki, J. Electrochem. Soc. 151 (4) (2004) A548–A557.
[27] K. Suzuki, H. Iwai, T. Nishino, in: B. Sunden, M. Faghri (Eds.), Transport Phenomena in Fuel Cells, WIT Press, UK, 2005, pp. 83–125.
[28] M. Sucipta, S. Kimijima, T.W. Song, K. Suzuki, ASME Paper FUELCELL2006-97013, 2006.